Bull. Mater. Sci., Vol. 33, No. 4, August 2010, pp. 469–474. © Indian Academy of Sciences.

Effect of SiO_3^{2-}/OH^- on plasma electrolytic oxidation of Ti–5Mo–4V–3Al

M ASADI[1,2,*], MEHDI ATTARCHI[1], M VAHIDIFAR[1,2] and A JAFARI[1]

[1]Materials Science and Engineering, Shahid Bahonar Kerman, Kerman, Iran
[2]Materials Science Department, Yazd Azad University, Yazd, Iran

MS received 9 July 2008; revised 31 July 2010

Abstract. Plasma electrolyte oxidation (PEO) was utilized to produce thick films on titanium and Ti–5Mo–4V–3Al alloys by immersing them in various solutions of Na_2SiO_3 and KOH with different concentrations to investigate the effect of SiO_3^{2-}/OH^- relations on the morphology and formed phases by utilizing SEM and XRD. Corrosion resistance is evaluated by open circuit potential (OCP) variation of samples in NaCl 3·5% and potentiodynamic polarization. The results show that the unstable film is formed by using more aggressive PEO electrolyte. By increasing this ratio, pore size varied from fine to coarse and the rate of corrosion decreased and OCP became more positive. The best protective film was formed in SiO_3^{2-}/OH^- ratio of 1.

Keywords. Corrosion; plasma electrolyte oxidation; titanium.

1. Introduction

Plasma electrolyte oxidation (PEO) is one of the most new attractive surface engineering techniques (Yerokhin *et al* 1999). PEO is capable of converting metallic titanium into a ceramic layer of titanium oxide at room temperature (Yerokhin *et al* 2002; Baszkiewicz *et al* 2005; Rudnev *et al* 2005; Yao *et al* 2008; Song *et al* 2009). This method was used for Al and its alloys (Wang *et al* 2009; Godja *et al* 2010), aluminum coatings (Wu *et al* 2007) and Mg alloys too (Duan *et al* 2007). PEO is usually done at high anodic potential (Yerokhin *et al* 1999). When discharge appears between samples, surface and electrolyte cause accelerated plasma in contrast to general anodic process (Yerokhin *et al* 1999, 2002). Rate of layer growth, which is one of the most important parameters of electrochemical behaviour of this process, is controlled by electrochemical and plasma thermochemical reactions (Yerokhin *et al* 2002; Duan *et al* 2007; Wu *et al* 2007). The structure of anodic film changed from amorphous to crystalline phase, e.g. anatase, brokite and rutile. This change is related to the breakdown potential, electrolyte concentration and surface temperature (Sul *et al* 2001; Yao *et al* 2008). In ordinary anodic oxidation in different solutions, a weak layer of hydrated amorphous oxide or TiO_2 (anatase) is produced which has weak corrosion resistance towards reduction acids and halogen solutions. When compared with anatase, rutile usually has better protective character. If the rutile or higher corrosion resistances is the aim of the process, the more controlled conditions must be used. For achieving these goals, choosing suitable solutions is of primary importance (Yerokhin *et al* 1999, 2000; Baszkiewicz *et al* 2005; Cao 2007).

To produce PEO coatings on titanium, alkaline electrolytes are widely used, which contain silicate, aluminates, phosphate and can passivate the metal surface due to the formation of insoluble compounds (Snizhko *et al* 2004).

The aim of this study was to achieve dense and protective coating on Ti and Ti–5Mo–4V–3Al by utilizing simple and available solution with a new aspect, ion concentration ratio.

2. Experimental

2.1 *Material and method*

Discs of Ti–5Mo–4V–3Al with 6·3 mm diameter and 5 mm thickness, were ground to 1000 grade by SiC papers and cleaned with acetone and distilled water. At first, OCP of each sample in the working electrolyte was measured vs calomel electrode (E = 0·2415 vs SHE) at room temperature, then the d.c. power supply was connected to make disc samples anode and stainless steel as cathode. The distance between electrodes was 3 cm. Different concentrations of sodium silicate and potassium hydroxide were used as working solution. The range of voltage and current, respectively 170–300 V and 0·001–6·3 A cm^{-2} (table 1) have been used for plasma electrolyte process. Voltage was increased with 100 V·min^{-1} and remained for 5 min in final recorded potential. The experiments were done at room temperature. After 5 min

*Author for correspondence (masadiz@gmail.com)

Table 1. PEO treatment regimes and film appearance.

Sample no.	Electrolyte	Spark voltage (V)	Current range (A/cm^2)	Appearance
1	Na_2SiO_3 : 20 g/L KOH : 5 g/L	245	0·005–0·37	Dark, rough light incorporations
2	Na_2SiO_3 : 20 g/L KOH : 10 g/L	160	0·001–1·2	Dark, light even
3	Na_2SiO_3 : 20 g/L KOH : 20 g/L	82	0·01–4·2	Light brown even
4	Na_2SiO_3 : 70 g/L KOH : 10 g/L	175	0·004–0·58	Dark, rough light, brittle
5	Na_2SiO_3 : 70 g/L KOH : 30 g/L	100	0·01–4·5	Dark, light even
6	Na_2SiO_3 : 70 g/L KOH : 70 g/L	50	0·66–6·3	Light brown even, light

Table 2. Surface potential of samples before and after PEO process.

Sample no.	Electrolyte	OCP measurement before plasma electrolyte treatment (mV vs SCE)	OCP measurement after plasma electrolyte treatment (mV vs SCE)
1	Na_2SiO_3 : 20 g/L KOH : 5 g/L	–604	–440
2	Na_2SiO_3 : 20 g/L KOH : 10 g/L	–635	–570
3	Na_2SiO_3 : 20 g/L KOH : 20 g/L	–650	–560
4	Na_2SiO_3 : 70 g/L KOH : 10 g/L	–700	+300
5	Na_2SiO_3 : 70 g/L KOH : 30 g/L	–695	+40
6	Na_2SiO_3 : 70 g/L KOH : 70 g/L	–800	–400

process the samples were cleaned with distilled water and then OCP was measured in the electrolyte at room temperature. Measured potentials vs SCE are illustrated in table 2.

2.2 *Morphology and XRD analysis*

A qualitative study of oxide film appearance was carried out visually. Conventional optical and scanning electron microscopy (SEM) techniques were employed to observe the film and surface morphology. Film phase composition was estimated using the X-ray diffractometer (CuK_α radiation) by scanning in the $2\theta = 20$ to 80 degrees by Philips® XPert model.

2.3 *Corrosion tests*

The corrosion resistance of formed films was evaluated by potentiodynamic tests by utilizing Autolab® PGSTAT30 system in 3·5% NaCl solution. The sample with an exposed area of 0·38 cm^2 was immersed into the solution and open circuit corrosion potential after 35 min was measured, and then the polarization test was conducted with 1 mV/s scan rate up to 1·5 V SCE (0·2415 vs SHE) approximately. All corrosion evaluation potentials were reported versus saturated calomel electrode.

3. Results and discussion

3.1 *Process characteristics of PEO and outward of formed film*

Figure 1 shows the behaviour of voltage–current curves in PEO experiments. When voltage is increased the rate of bubble formation increased simultaneously, until covering the whole anode. The break in voltage diagram and spark formation on anode surface happened at the same time. Whenever hydroxyl ions concentration was raised,

the amount of spark also boosted (Asadi *et al* 2010). It is known that most of cell voltage (power) is consumed for overcoming the resistance of growing oxide film thus voltage–current pattern defines film growth. As a first step, 1 to 3 min after switching d.c. power supply, until the breakdown of oxide film, the current shows linear raise with increasing voltage. At this point film thickness and therefore, electrical resistance of film varies slightly which is the result of passivity effect of the electrolyte (Yerokhin *et al* 2000; Asadi *et al* 2010). The situation which is shown in figure 1b is related to the more corrosive solutions than figure 1a where achieving passivation is much more difficult. In more corrosive media the current increases faster with more fluctuations. According to Inho Han's report, increasing OH^- ions in electrolyte causes decrease in potential of breakdown and sparking voltage (Han *et al* 2007; Asadi *et al* 2010). In the maximum current density, the film breaks down that indicates the discharging of sample's surface in a short time interval. Stable sparking depending on solution concentration occurs between 175 and 300 V. Increasing resistance after a while causes increase in voltage applied whereas current density decreases. Increasing of resistance is as a result of surface layer thickening and phase transformation. Table 1 shows effect of electrolyte on voltage–current characteristics and macroscopic appearance of oxide films. An electrolyte which consists of silicate with KOH shows most severe sparking and highest range of voltage. Further XRD analysis, as shown in §3.3, shows the white compounds in the film are amorphous silicate deposits in the discharging canals.

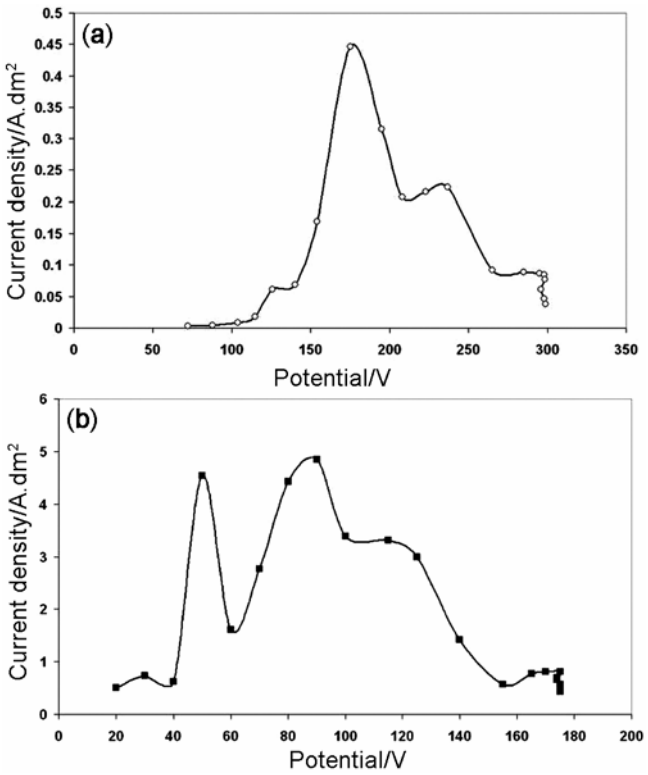

Figure 1. Voltage–current behaviour of PEO process in (**a**) Na_2SiO_3 70 g·l^{-1} and KOH 10 g·l^{-1} and (**b**) Na_2SiO_3 70 g·l^{-1} and KOH 70 g·l^{-1}.

3.2 *SEM analysis*

Most amorphous silicate coatings formed on Ti alloys through PEO process are uneven and porous (Wang *et al* 2005). This is illustrated in figures 2 and 3. Mean pore diameter in 70 g·l^{-1} silicate solutions (figure 4) changes from 7·7 μm, 7·6 μm to 4 μm for 30 g/L, 50 g/L and 70 g·l^{-1} KOH, respectively but mean pore diameter changes for 20 g·l^{-1} from 9.4 μm, 7·1 μm to 7·6 μm for 5 g·l^{-1}, 10 g·l^{-1} and 20 g·l^{-1} KOH, respectively. In both cases mean pore diameter decreased with an increase in KOH concentration. In ion concentration ratio point of view, some more different schemes appeared. In lower base concentration and lower Na_2SiO_3/KOH ratio, mean diameter decreased slowly but diameter distribution decreased rapidly. In higher concentration (both Na_2SiO_3 and KOH), mean diameter of pores decreases faster than lower ones, which is depicted in figure 4a. Moreover, diameter distribution decreased more slowly than the previous case which implied less homogeneity in higher concentration.

The surface of sample when plasma oxidized in concentration ratio, 1 (20/20 and 70/70 SiO_3^{2-}/OH^-), show the most uniform surface rather than the other concentration ratio. The highest concentration (70/70 SiO_3^{2-}/OH^-) shows more number of pores than the lower one. Moreover, the absence of crack or micro crack at this ratio indicates softer and more ductile coating. The changes in topology of the sample surface could be a result of recrystallization but it needs further evaluation.

3.3 *Phase compositions*

As is shown in figure 5, with increasing KOH concentration and decreasing SiO_3^{2-}/OH^- ratio in 20 g·l^{-1} SiO_3^{2-} concentrations, the rutile phase appeared, in addition to the anatase phase, which is present in both cases. At this concentration, 20 g/L SiO_3^{2-}, silicate phase disappeared by achieving ion ratio, one. In highest ion concentration (figure 6), rutile and silicate in both cases were formed. Comparison between 5b and 6b, which have same ions ratio, illustrate that in lower ion concentration rutile predominantly formed but by increasing the ion concentrations, complex structure containing rutile, anatase and silicate formed.

3.4 *Corrosion resistance evaluation*

The protective effect of oxide films formed on titanium alloys is basically conditioned by (i) shifting of open circuit potential; (ii) suppression of activity of aggressive

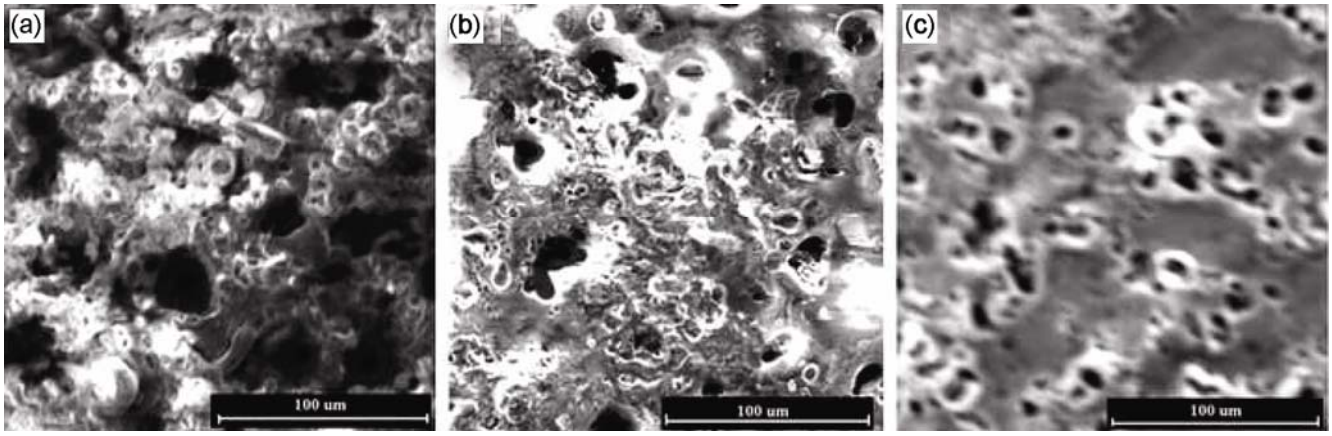

Figure 2. SEM of oxide film in 20 g·l^{-1} Na_2SiO_3 and (**a**) 5 g·l^{-1} KOH, (**b**) 10 g·l^{-1} KOH and (**c**) 20 g·l^{-1} KOH.

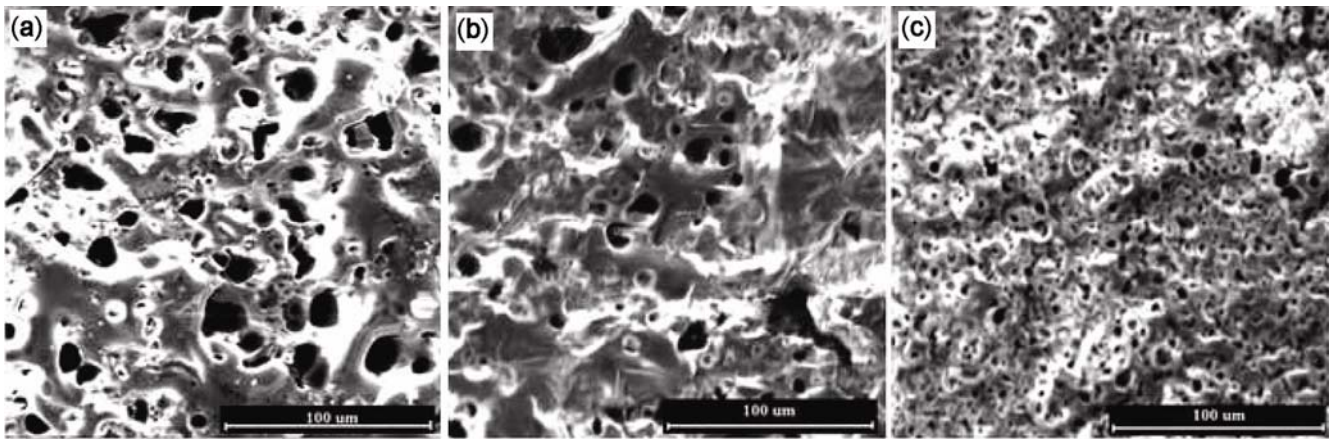

Figure 3. Morphology of oxide films in electrolyte, 70 g·l^{-1} Na_2SiO_3 and (**a**) 30 g·l^{-1} KOH, (**b**) 50 g·l^{-1} KOH and (**c**) 70 g·l^{-1} KOH.

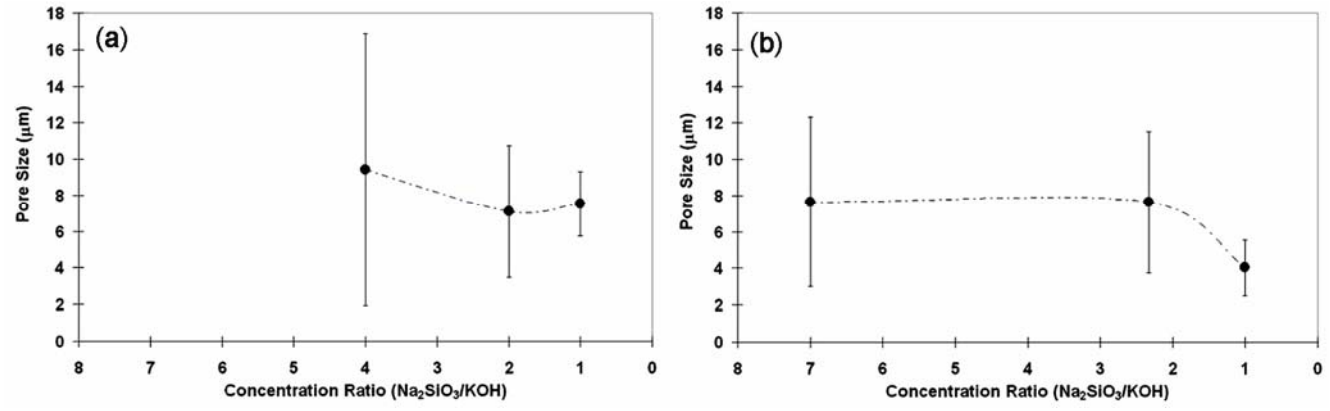

Figure 4. Mean pore diameter vs ions concentration ratio (**a**) 20 g·l^{-1} Na_2SiO_3 and (**b**) 70 g·l^{-1} Na_2SiO_3.

ions adsorbed and (iii) reduction of charge-carrier mobility particles at the metal–electrolyte interface. All these items in a complicated way depend on combination of characteristics of the oxide film and corrosive environment. Thereby, the PEO technique providing possibilities for the variation of composition, structure and thickness of the surface oxide film, so enhanced possibilities for the corrosion protection of Ti alloy (Yerokhin *et al* 2000). Table 2 shows the open circuit potential of samples before and after process in designated solution. With

increasing SiO_3^{2-}/OH^{-1} (samples 3 to 1 and 6 to 4), surface potential became much more positive. So it provides better chemical stability for alloy. The most negative surface potential, less thermodynamic tendency to corrosion, occurs for $SiO_3^{2-}/OH^{-1} = 1$.

Figures 7 and 8 shows anodic potentiodynamic polarization for sample with formed films due to process and Ti base alloy without any coating in NaCl 3·5%. Formed oxide films could transform corrosion potential to positive values and thus alloy could resist to corrosion. It means that the formed film has less thermodynamic tendency to corrosion. Figure 7c shows that film in electrolyte at SiO_3^{2-}/OH^- ratio of 20/5 transform corrosion potential to 0·2 V. With increasing OH^- ion in solution, corrosion potential decreases to –0·2 V. Passivity current, I_{PP}, in the film forming in electrolyte at SiO_3^{2-}/OH^- ratio of 20/5 was less than SiO_3^{2-}/OH^- ratio of 20/20 (figure 7b) but anodic slope is changed because of high porous oxide film. The more porous film could cause reduction in stability of film. This change in slope is not observed for electrolyte with 70 g/L SiO_3^{2-}. This behaviour is related to the thicker and denser structure of film formation, which could separate sample surface from corrosive environment, in the higher concentration. Corrosion potential goes to negative values with decrease of SiO_3^{2-}/OH^- ratio.

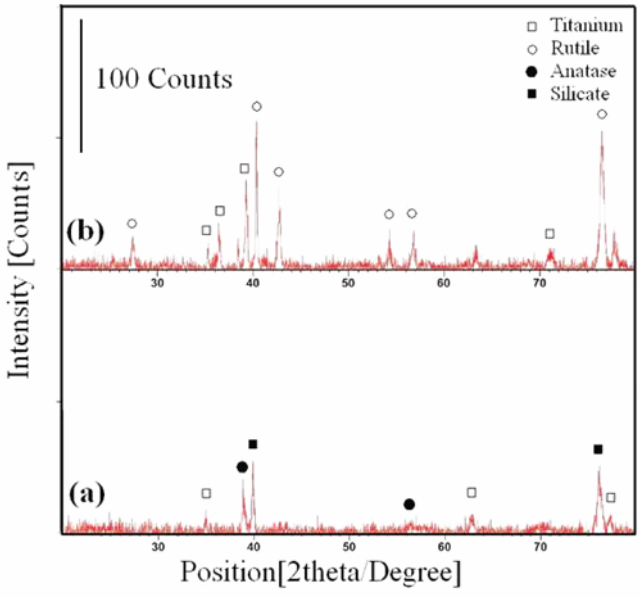

Figure 5. XRD patterns of oxide film in electrolyte 20 g·l^{-1} Na_2SiO_3 with (**a**) 5 g·l^{-1} KOH and (**b**) 20 g·l^{-1} KOH.

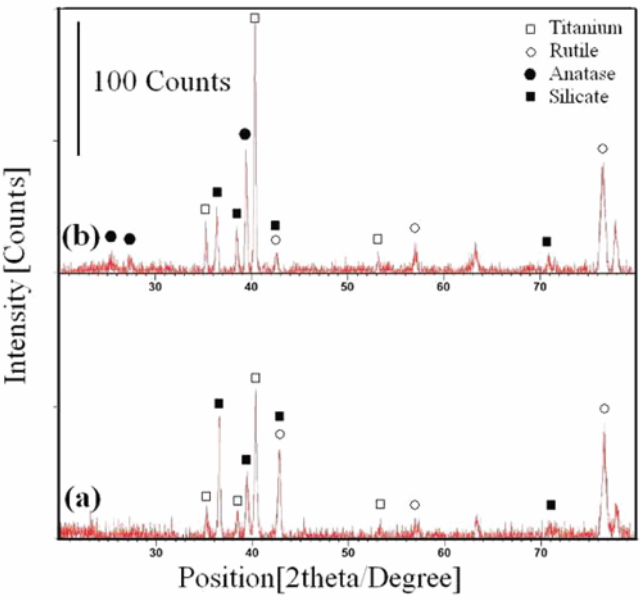

Figure 6. XRD patterns of oxide film in electrolyte 70 g·l^{-1} Na_2SiO_3 with (a) 30 g·l^{-1} KOH and (b) 70 g·l^{-1} KOH.

4. Conclusions

(I) By increasing aggressive ion in PEO electrolyte, unstable films growth is detected.
(II) Surface morphology in all cases was porous and mean diameter of pores decreased by reduction in SiO_3^{2-}/OH^-. The most even film is gained in highest SiO_3^{2-}/OH^-,

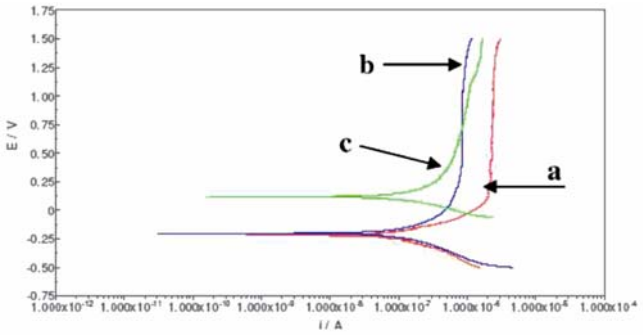

Figure 7. Corrosion potentiodynamic curves of PEO films exposed in 3·5% NaCl (a) substrate, (b) 20 g·l^{-1} Na_2SiO_3, 20 g·l^{-1} KOH and (c) 20 g·l^{-1} Na_2SiO_3, 5 g·l^{-1} KOH.

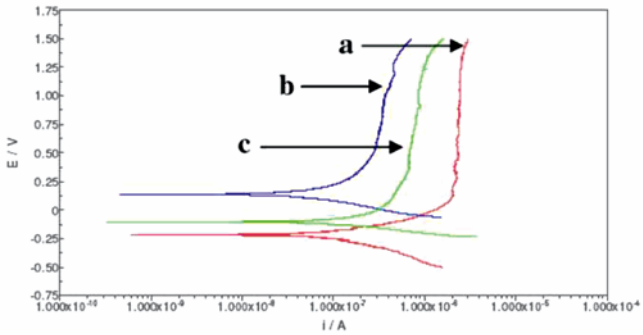

Figure 8. Corrosion potentiodynamic curves of PEO films exposed in 3·5% NaCl (a) substrate, (b) 70 g·l^{-1} Na_2SiO_3, 30 g·l^{-1} KOH and (c) 70 g·l^{-1} Na_2SiO_3, 70 g·l^{-1} KOH.

one in both cases, however, in 70/70 ratio, higher pore density could be seen.

(III) In lower ion concentration, rutile predominantly formed but by increasing the ion concentrations, complex structure which contains rutile, anatase and silicate will be formed.

(IV) The highest SiO_3^{2-}/OH^- ratio shows better corrosion resistance due to their thicker surface film with rutile phase. Both corrosion potential, thermodynamic tendency, and polarization, kinetically, approved this behaviour.

References

Asadi M, Attarchi M, Vahidifar M and Jafari A 2010 *Defect and Diffusion Forum* **297–301** 1167

Baszkiewicz J, Krupa D, Mizera J, Sobczak J W and Bilinski A 2005 *Vacuum* **78** 143

Cao Fa-he, Cao J-l, Zhang Z, Zhang J -Q and Cao C-n 2007 *Mater. Corros.* **58** 696

Duan H, Yan C and Wang F 2007 *Electrochimica Acta* **52** 3785, 5002

Godja N, Kiss C, Locker A, Schindel A, Gavril J, Wosik R and Mann J 2010 *Tribol. Int.* **43** 1253

Han I, Choi J H, Zhao B H, Baik H K and Lee I-S 2007 *Curr. Appl. Phy.* **7** e23

Rudnev V S, Vasilyeva M S, Kondrikov N B and Tyrina L M 2005 *Appl. Surf. Sci.* **252** 1211

Snizhko L O, Yerokhin A L, Pilkington A, Gurevina N L, Misnyankin D O, Leyland A and Matthews A 2004 *Electrochim. Acta* **49** 2085

Song H, Park S, Joeng S and Park Y 2009 *J. Mater. Process. Technol.* **209** 864

Sul Y-T, Johansson C B, Jeong Y and Albrektsson T 2001 *Med. Eng. Phys.* **23** 329

Wang K, Koo B, Lee C, Kim Y, Lee S and Byon E 2009 *T. Nonferr. Metal. Soc.* **19** 866

Wang Y M, Jiang B L, Lei T Q and Guo L X 2005 *Appl. Surf. Sci.* **246** 214

Wu Z, Xia Y, Li G and Xu F 2007 *Appl. Surf. Sci.* **253** 8398

Yao Z, Jiang Y, Jia F, Jiang Z and Wang F 2008 *Appl. Surf. Sci.* **254** 4084

Yerokhin A L, Nie X, Leyland A, Matthews A and Dowey S J 1999 *Surf. Coat. Technol.* **122** 73

Yerokhin A L, Nie X, Leyland A and Matthews A 2000 *Surf. & Coat. Technol.* **130** 195

Yerokhin A L, Leyland A and Matthews A 2002 *Appl. Surf. Sci.* **200** 172